JOURNAL OF SOLID STATE CHEMISTRY 76, 178–185 (1988)

The Magnetic Susceptibility of Pr^{4+} in $BaPrO_3$: Evidence of Long-Range Magnetic Order*

M. BICKEL, G. L. GOODMAN, AND L. SODERHOLM†

Chemistry Division, Argonne National Laboratory, Argonne, Illinois 60439

AND B. KANELLAKOPULOS

Heisse Chemie, Kernforschungszentrum, Karlsruhe, D 7500 Karlsruhe, West Germany

Received October 28, 1987; in revised form April 8, 1988

We have reexamined the magnetic behavior of $BaPrO_3$ in the temperature range $4.2 < T < 300$ K. An anomaly in the susceptibility at 11.6(1) K has been observed, and is attributed to the onset of long-range ordering of the Pr^{4+} f-electrons. Above the critical temperature, the paramagnetism is composed of a temperature-dependent term with an effective moment of 0.7(1) μ_B and a temperature-independent term of $6.9(2) \times 10^{-4}$ emu/mole. Calculations based on a simple crystal field model explain the low effective moment found experimentally. © 1988 Academic Press, Inc.

Introduction

Considerable interest has centered on the elucidation of systematics in the magnetic behavior of $5f$ ions in binary or ternary oxides (*1–9*). The current attention is focused on the interaction between f-electrons in a variety of ternary oxides which share as a common structural feature two- or three-dimensional networks of corner-sharing $M–O_6$ octahedra. Within this class, the perovskite (ABO_3) structure is of particular interest, since it is known to stabilize a large number of ions in a variety of oxidation states. Focusing on the case in which A is a divalent ion (A = Sr, Ba), this structure can accommodate a variety of tetravalent lanthanide and actinide ions (*10–17*) at the B site. This B-ion sits at the center of the slightly distorted octahedron formed by the six near-neighbor oxygen atoms. The octahedra are linked in a 3-d corner-sharing network which can act as a superexchange pathway, permitting interactions between the B-ions through the intervening oxygen atoms. These interactions effect the magnetic behavior of the metal ions, permitting long-range ordering of the unpaired f-moments.

Light tetravalent actinide ions which are stabilized in the perovskite structure appear to order magnetically at relatively high temperatures. For example, $BaNpO_3$ orders at 48 K (*2*) and $BaPuO_3$ orders at 160 K (*18*). There are two magnetic lanthanide

* The U.S. Government's right to retain a nonexclusive royalty-free license in and to the copyright covering this paper, for governmental purposes, is acknowledged.

† To whom correspondence should be addressed.

0022-4596/88 $3.00

TABLE I

THE LATTICE PARAMETERS OF $BaPrO_3$ AS DETERMINED BY NEUTRON DIFFRACTION (REF. (*21*)) AND X-RAY DIFFRACTION (REF. (*12*) AND THIS WORK) OF POWDER SAMPLES

$BaPrO_3$	Ref. (*21*)	Ref. (*12*)	This work
a (Å)	6.181(1)	6.181	6.170(2)
b (Å)	6.214(1)	6.210	6.214(3)
c (Å)	8.772(1)	8.728	8.716(3)

ions which form in this structure, Pr^{4+} and Tb^{4+}. $BaTbO_3$ orders at 37 K (*19*) but $BaPrO_3$ has been reported to show no evidence of magnetic order down to 2 K (*19*). We found this lack of magnetic ordering in $BaPrO_3$ surprising in light of the relatively high ordering temperatures found for the other tetravalent ions in this compound. Therefore, we set out to reinvestigate the magnetic behavior of $BaPrO_3$ in an attempt to understand the apparently inconsistent behavior of Pr^{4+} in this host.

Experimental Section

The samples were prepared by repeatedly grinding and firing to 1000°C mixtures of dried $BaCO_3$ (p.a., Merck, West Germany) and Pr_6O_{11} (99.999% EGA-Chemie, West Germany) in the correct stoichiometric metal ratios. $BaPrO_3$ was prepared and stored in atmospheres with different oxidative powers, the details of which are described elsewhere (*6*). The samples were characterized by Cu$K\alpha$ X-ray diffraction from a Scintag PADV diffractometer calibrated with NBS Si powder. The sample used for the magnetic measurements is $BaPrO_{3.03(3)}$, as determined by iodometric titration (*20*). In view of the error limits for this analysis, these results seem entirely consistent with the ideal perovskite stoichiometry and therefore we use the formula $BaPrO_3$ to describe our sample. Infrared spectra of the compounds as KBr-pellets were obtained with a Perkin–Elmer M283 device (4000 to 200 cm^{-1}) and as polyethylene pellets with a Beckman FS-729 spectrometer (40 to 400 cm^{-1}). Magnetic susceptibility measurements from 300 to 4.2 K were performed on a Faraday balance (*6*).

Results and Discussion

Structure

All of the peaks observed by X-ray powder diffraction for $BaPrO_3$ were indexed using an orthorhombic cell and indicated a single phase material within the accuracy of the measurement (approx. 5%). The lattice constants refined from these data are listed in Table I and are consistent with the previous values obtained from neutron diffraction where $BaPrO_3$ was found to crystallize as an orthorhombically distorted perovskite (*21*).

The ideal perovskite ABO_3, typified by the cubic compound $CaTiO_3$ (*10*), can be viewed as a three-dimensional network of Ti–O corner-sharing octahedra, with the *B*-ion sitting in a site of $m3m$ (O_h) symmetry. The orthorhombic distortion observed in the Pr compound involves a cooperative buckling of these corner-sharing octahedra, as shown in Fig. 1 and as typified by $GdFeO_3$ (*22*). This buckling involves a reorientation of the *B*–O octahedra with respect to each other, which results in a drop of the crystal symmetry from cubic ($Pm3m$) to orthorhombic ($Pnma$), and the local site symmetry at the *B* cation drops from $m3m$ to $\bar{1}$. However, while there is a cooperative buckling of octahedra with respect to each other, there are only small changes in the near-neighbor oxygen coordination about the *B* site. In $BaPrO_3$ the Pr^{4+} ions have an almost octahedral arrangement of near-neighbor oxygens, with Pr–O distances of 222 and 223 pm. The Ba–O distances range from 258 to 363 pm (*21*).

Information about the effective site symmetry of the Pr^{4+} in $BaPrO_3$ can also be

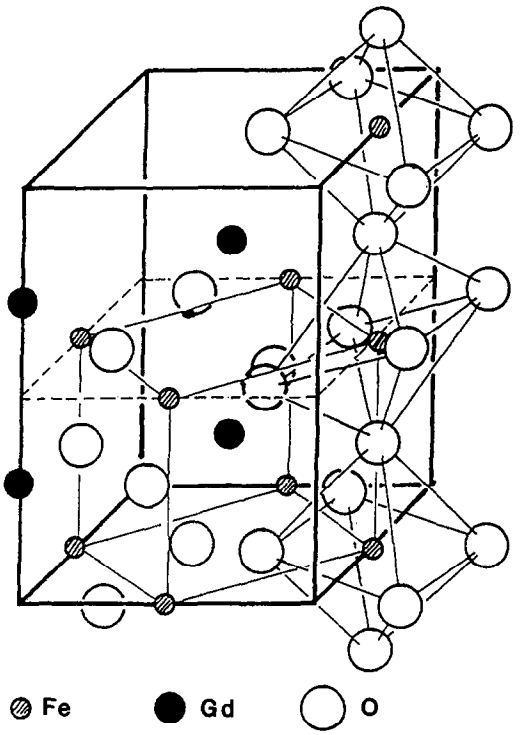

FIG. 1. Orthorhombic perovskite ($GdFeO_3$) structure. The Pr–O–Pr superexchange pathway can be viewed as corner-linked $Pr–O_6$ octahedra.

inferred from the infrared spectrum of this material, which is shown in Fig. 2. Comparison of this figure with the spectra for the cubic, tetragonal, orthorhombic, and rhombohedral phases of $BaTiO_3$ (*23*) suggests only small departures from octahedral site symmetry in the present case. The same conclusion follows from comparison with other work on perovskite titanates (*24*). The relationship between infrared frequencies observed here and those reported for orthorhombic $CaTiO_3$, cubic $SrTiO_3$, and tetragonal $PbTiO_3$ (*24*) supports our hypothesis of nearly octahedral geometry for the site of the Pr ion in $BaPrO_3$.

Magnetic Susceptibility (χ)

A Curie plot (χ^{-1} vs T) of the magnetic susceptibility data, obtained on powdered samples of $BaPrO_3$, is shown in Fig. 3. The anomaly in the data at 11.6(1) K is interpreted as evidence of long-range magnetic ordering of the Pr^{4+} moments. This finding is consistent with the ordering temperatures in other compounds with *f*-ions on the *B*-site of the perovskite lattice. It is also similar to the ordering temperature in PrO_2 (14 K) (*25*), another Pr^{4+} compound with Pr–O–Pr pathways available for superexchange.

Previously, $BaPrO_3$ was studied by neutron diffraction and magnetic susceptibility (*19*) where there was no evidence found for long-range order, and there was no anomaly in the inverse susceptibility data at about 12 K. The difference between the previous work and the results presented here may be the result of slight differences in oxygen stoichiometry. The presence of small quantities of Pr^{3+} may be expected depending on the method of sample prepa-

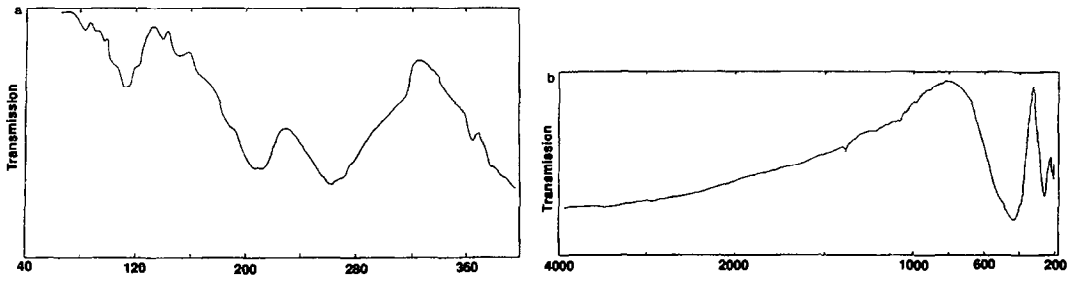

FIG. 2. The infrared spectra of $BaPrO_3$ from (a) 400 to 40 cm^{-1} and from (b) 4000 to 200 cm^{-1}.

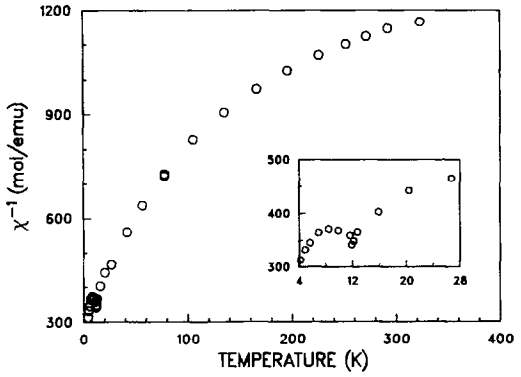

FIG. 3. A Curie plot, χ^{-1} vs T, from a powdered sample of $BaPrO_3$, with a notable cusp at 11.6(1) K which marks the onset of long-range order.

ration and storage (*6*). The incorporation of Pr^{3+} is accompanied by oxygen defects, required for charge balance, and may result in sufficient defect concentration to destroy any cooperative magnetic ordering (*26*).

We believe that the deviation from the observed Curie Law behavior is primarily the result of a temperature-independent contribution to the paramagnetism (TIP), since a plot of χT vs T (Fig. 4) is rectilinear above 100 K. If a χ_{TIP} term is added to the Curie Law, the slope of this χT curve equals the TIP contribution, and the intercept is proportional to the effective moment. Since the Pr^{4+} moments order at about 12 K, the addition of a Weiss constant to the Curie Law is justified. However, the inclusion of a Weiss constant of -12 K into our data analysis does not significantly alter either the effective moment or the TIP contribution obtained from these data. Therefore, assuming no Weiss constant, the effective moment for Pr^{4+} in $BaPrO_3$ determined from Fig. 4 is 0.7(1) μ_B, with a TIP contribution of 6.9(2) $\times$ 10^{-4} emu/mole.

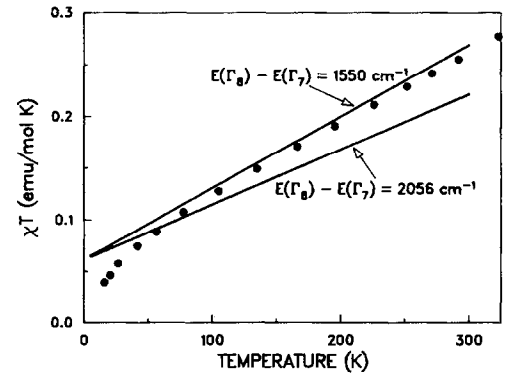

FIG. 4. A plot of χT vs T for $BaPrO_3$ (solid circles). The slope is equal to the temperature-independent paramagnetism, and the intercept is proportional to the effective moment. Also shown are the curves calculated for $E(\Gamma_8) - E(\Gamma_7) = 2056$ and 1550 cm^{-1}.

The observed effective moment, 0.7(1) μ_B, is much smaller than expected for an f^1-free ion in its $J = \frac{5}{2}$ ground state, 2.54 μ_B, and there is a large TIP contribution to the measured susceptibility. These results suggest that the crystalline electric field (CEF) has a significant effect on the magnetic properties. In order to investigate the effect of the CEF on the susceptibility of Pr^{4+} in $BaPrO_3$, we have used an octahedral point charge model to calculate the susceptibility as a function of temperature. In our initial attempts to model the data, we utilized the Stevens formalism (*27*), a common method of treating Ln^{3+} magnetic data. This formalism only considers the states arising from the $^2F_{5/2}$ ground term, and ignores all contributions arising from the excited $^2F_{7/2}$ state, approximately 3000 cm^{-1} above the ground term, based on the free-ion spin–orbit splitting (*28*). In pure O_h symmetry the $^2F_{5/2}$ ground multiplet splits into a Γ_7-ground state and a Γ_8-excited state. The Γ_7-ground state is a Kramers doublet and cannot be further split by the crystal field so the first excited state is derived from this Γ_8 quartet. On the basis of inelastic neutron scattering experiments the first excited state has been located at approximately 2000 cm^{-1} above the Γ_7 (*29*). The Γ_8-quartet can be split by lower site symmetry, and its energy strongly influenced by the magnitude of both fourth degree and sixth degree CEF components. This means that the calcu-

lated TIP, which arises from a mixing of the ground and excited state wavefunctions by the magnetic field will be sensitive to the model chosen for the CEF.

Within $J = \frac{5}{2}$ states, the octahedral Hamiltonian using Stevens' notation (*27*) takes the form:

$$H_{CEF} = A_4\langle r^4\rangle\beta(O_4^0 + 5O_4^4) + A_6\langle r^6\rangle\gamma(O_6^0 - 21O_6^4), \quad (1)$$

where the O_l^m's are related to the spherical harmonics (*30*), and $\langle r^n\rangle$'s are the radial integrals for the rare-earth electrons (*31*). β and γ are the Stevens factors for the reduced matrix elements $\langle J\|\Theta\|J\rangle$, $\Theta = 2, 3$. γ is identically zero, while β is nonzero for f^1 systems in this formalism. Thus, only one variable parameter, $A_4\langle r^4\rangle$ controls the CEF. An estimate of this parameter (965 cm^{-1}) is available from inelastic neutron scattering data on $BaPrO_3$ (*29*), and was used to calculate the eigenfunctions and eigenvalues of Pr^{4+} in this compound. The susceptibility can then be calculated using the van Vleck formalism (*8, 32*). The curvature to the experimental data is reproduced by the calculation, but the magnitude of the computed susceptibility is much larger than found by experiment. The effective moment extracted from this calculation is 1.23 μ_B and it is independent of the size of the crystal field. Although this value is smaller than the free ion effective moment (2.54 μ_B), it is still significantly larger than the observed value, 0.7 μ_B. On the other hand χ_{TIP} is calculated to be 3.8×10^{-4} emu/mole, about half the experimental value, $6.9(2) \times 10^{-4}$ emu/mole.

We have tried in two ways to bring the calculated TIP value in this model closer to the experimental value while retaining the Stevens formalism. In the first approach an axial term is added to the octahedral Hamiltonian. In order to reduce the number of new parameters we have added only one axial $A_2\langle r^2\rangle$ term while preserving the cubic relation of the fourth-order terms and keeping the magnitude of $A_4\langle r^4\rangle$ fixed at the value obtained by neutron inelastic scattering (*29*). This type of axial field causes a *decrease* in the calculated TIP term. However since the calculated TIP contribution was already too small, an axial distortion introduced in this manner does not help to reproduce the experimental results. Furthermore, the infrared results suggest that the site symmetry is well represented as cubic. In the second approach the octahedral symmetry is retained but the value of $A_4\langle r^4\rangle$ is reduced to 725 cm^{-1} in order to reproduce the χ_{TIP} experimental value. However, in this case the calculated effective moment remains unchanged and there is no other experimental data suggesting a crystal field value this low.

The Stevens formalism, commonly used to treat data obtained from trivalent lanthanides, does not produce useful results for this case of Pr^{4+}. The basic assumption of the method, namely, that only states arising from the $^2F_{5/2}$ ground term need to be considered in the calculation, is false in this case. The effect of the crystal field is not small with respect to that of the spin–orbit coupling, and the CEF splitting of the $^2F_{5/2}$ ground term (2000 cm^{-1}) is actually comparable to the spin–orbit splitting of the free ion $^2F_{5/2}$ and $^2F_{7/2}$ terms (3000 cm^{-1}), so that significant mixing of all these states occurs.

In order to better understand this problem, we have also done a full intermediate coupling crystal-field calculation involving all 14 states arising from f^1. The Hamiltonian for this octahedrally symmetric case is specified by three energies: a spin–orbit coupling and the two crystal field energies. There are several possible ways in which to define these two crystal field energies. The most appropriate choice depends on the details of the situation under investigation. Often when the effect of the crystal field is small and the emphasis is on its relationship to the surrounding crystal structure, it is

desirable to use one energy parameter each for the fourth and the sixth order tensor operators representing the electric field in the crystal. These parameters are often called $A_4\langle r^4\rangle$ and $A_6\langle r^6\rangle$ as in (*29*). In a case like the present one, however, it is more convenient to focus on the energy of separation between the *f*-electron states in the absence of spin–orbit coupling, which is analogous to 10 Dq in the transition metal cases (*33*). Then, the two ligand field parameters may be written (*34*)

$$7R = E(^2t_{2u}) - E(^2a_{2u})$$

and

$$7Q = E(^2t_{1u}) - E(^2t_{2u}),$$

where $E(^2\Gamma)$ stands for the energy of the *f*-electron states transforming as the $\Gamma(= a_{2u}, t_{1u}$, or $t_{2u})$ representation of O_h. These two sets of parameters are related as follows:

$$A_4\langle r^4\rangle = 21(3Q + 2R)/32$$

$$A_6\langle r^6\rangle = 39(5Q - 4R)/640$$

or

$$7R = 80(13A_4\langle r^4\rangle - 84A_6\langle r^6\rangle)/429$$

$$7Q = 64(13A_4\langle r^4\rangle + 70A_6\langle r^6\rangle)/429.$$

The magnetic moment of the Γ_7 states for an *f*-electron in an octahedrally symmetric field can be written as

$$\boldsymbol{\mu}_{\text{eff}} = \mu_B g' \mathbf{s}'$$

in terms of the Bohr magneton μ_B, an effective spectroscopic splitting factor g′ and the Pauli spin matrices

$$\mathbf{s}' = \frac{1}{2}\begin{pmatrix} \mathbf{k} & \mathbf{i} - \mathbf{ij} \\ \mathbf{j} + \mathbf{ij} & -\mathbf{k} \end{pmatrix}.$$

The value of g′ for the ground Γ_7 state of f^1 is completely determined by the ratio of the crystal field energy R to the spin–orbit coupling constant ζ_f, where $E_{S\text{-}O} = \zeta_f \mathbf{l} \cdot \mathbf{s}$.

Let

$$a = \tfrac{1}{4}\{1 - 14(R/\zeta_f) + 7[1 - (4R/7)\zeta_f + 4(R/\zeta_f)^2]^{1/2}\}$$

then (*35*)

$$g' = (6 - 8a)/(a^2 + 3).$$

Using $|\mu_{\text{eff}}| = 0.7(1)\ \mu_B$ we find

$$g' = \pm 0.7(1) \times 2/[3]^{1/2} = \pm 0.808(0.115)$$

leading to three possible values for $R/(|R| + \zeta_f)$: −0.54, 0.205, or 0.50. The value of 0.205 seems most reasonable yielding $7R$ = 1562 cm^{-1} when combined with ζ_f = 865 cm^{-1} from the atomic spectrum of Pr^{4+} in the vapor phase (*28*). (It seems worth noting that this electronic structure yields a negative value for g′, a prediction that may be investigated using polarized microwave radiation as was done for NpF_6 by Hutchison and Weinstock (*36*).) We reject the other two possible values for $7R$ because one is negative (the one corresponding to −0.54) requiring the a_{2u} state to be at higher energy than the t_{2u} states, which is appropriate in cubic but not octahedral coordination, and the other is approximately 6000 cm^{-1}, much larger than the crystal field splitting expected for a rare-earth ion like Pr^{4+}.

Combining the foregoing values for ζ_f and $7R$ with the assigned value of 2057 ± 81 cm^{-1} for the transition energy from the ground Γ_7 states to the first excited Γ_8 states as seen in inelastic neutron scattering (*29*), we obtain $7Q$ = 2881 ± 100 cm^{-1}. When these values of ζ_f, $7R$, and $7Q$ are used, the energy levels shown in Table II are obtained for the f^1 configuration. Putting these energy levels and their corresponding magnetic matrix elements into the van Vleck expression for paramagnetism (*8, 32*) yields the calculated curve plotted in Fig. 4. In this analysis, the effective moment, 0.69 μ_B, can be fitted to agree with the value obtained experimentally. The temperature-

TABLE II

THE CALCULATED ENERGY LEVELS OBTAINED FOR THE f^1 CONFIGURATION OF Pr^{4+} IN $BaPrO_3$ FOR (1) $\zeta_f = 865$, $7R = 1562$, AND $7Q = 2881$ AND (2) $\zeta = 865$, $7R = 1562$, AND $7Q = 1267$ (ALL NUMBERS ARE IN cm^{-1})

	Calculated energies	
Symmetry	(1)	(2)
Γ_7	0	0
Γ_8	2056	1551
Γ_7	3202	3202
Γ_8	5589	4480
Γ_6	6776	5162

independent term is then calculated to be 5.34×10^{-4} emu/mole as compared to our interpretation of the data to yield 7×10^{-4} emu/mole. The agreement seems quite reasonable in light of uncertainties associated with the required Selwood diamagnetic correction (*37*) and the simplicity of the octahedral crystal field model used here. It should be noted that the experimental magnetic susceptibility above 100 K can be fit very well in terms of an energy difference $E(\Gamma_8) - E(\Gamma_7)$ of 1550 cm^{-1} rather than 2056 cm^{-1} and the corresponding curve is plotted in Fig. 4 as well. There is however no reason to assign a state at this lower energy. The much more likely explanation is that the discrepancy in χ_{TIP} is due to the uncertainties of the diamagnetic correction (*37*) and the limitations of the cubic crystal model.

It is informative to contrast the two crystal field calculations performed here. The first calculation considers only states arising from the ground $^2F_{5/2}$ term and ignores the states arising from $^2F_{7/2}$. Considering only these states is a common practice when dealing with trivalent rare-earth ions. However, this assumption is not valid for tetravalent praeseodymium in $BaPrO_3$; instead the CEF and spin–orbit parameters are comparable. Considering the simplified model, and assuming octahedral symmetry, the effective magnetic moment for the Γ_7 level derived from $^2F_{5/2}$, is fixed at 1.24 μ_B, independent of the size of the CEF. It is only by including states arising from the excited $^2F_{7/2}$ term that the calculated magnetic moment can be altered. A small amount of mixing can have a large effect on the effective moment and the TIP term. Consequently the crystal field parameter obtained by ignoring $^2F_{7/2}$ states ($A_4\langle r^4\rangle = 725$ cm^{-1}) is quite different from those obtained with the inclusion of these states ($A_4\langle r^4\rangle = 1100$ cm^{-1}; $A_6\langle r^6\rangle = 71$ cm^{-1}), with the latter adequately reproducing the experimental susceptibility above 100 K.

Conclusions

We have studied the magnetic properties of $BaPrO_3$ in the temperature range $4.2 < T < 300$ K. We find an anomaly in the χ^{-1} vs T curve at 11.6(1) K which is interpreted as the onset of long-range order of the Pr^{4+} moments. The curvature in the χ^{-1} vs T data above 70 K is shown to be the result of second-order, temperature-independent paramagnetism. A comparison of crystal field calculations using the Stevens formalism with those of a full intermediate coupling scheme clearly demonstrates that only a full calculation, which deals with all the states arising from the f^1 configuration, is able to reproduce the experimental findings. The inability of the simplified calculations to reproduce the experimental effective moment demonstrates that the simplified calculations often used to determine the CEF in trivalent rare earths are not satisfactory in this case. The good agreement between the magnetic susceptibility calculated using all the energy levels and the experimental data available for Pr^{4+} in $BaPrO_3$ is consistent with our ultimate aim in performing these calculations, that

is, to provide eigenfunctions and eigenvalues of Pr^{4+} which can be transferred to other systems and other experiments.

Acknowledgments

The authors thank W. T. Carnall for helpful discussions. This work was supported by the U.S. Department of Energy, BES-Chemical Sciences under Contract W-31-109-ENG-38. One of us (M.B.) thanks NATO for a Postdoctoral Fellowship.

References

1. B. KANELLAKOPULOS, E. HENRICH, C. KELLER, F. BAUMGARTNER, E. KONIG, AND V. P. DESAI, *Chem. Phys.* **53,** 197 (1980).
2. B. KANELLAKOPULOS, C. KELLER, R. KLENZE, AND A. H. STOLLENWERK, *Physica B* **102,** 221 (1980).
3. E. KONIG, C. RUDOWICZ, V. P. DESAI, AND B. KANELLAKOPULOS, *J. Chem. Phys.* **78,** 576 (1983).
4. T. KRUGER, H. APPEL, H. HAFFNER, AND B. KANELLAKOPULOS, "Applications of the Mössbauer Effect" (Y. Kagan and I. S. Lyobutin, Eds.), Vol. 2, Gordon & Breach, New York (1983).
5. M. BICKEL, S. GEGGUS, H. APPEL, H. HAFFNER, AND B. KANELLAKOPULOS, *J. Less-Common Met.* **121,** 291 (1986).
6. M. BICKEL, KFK-4109, Kernforschungszentrum, Karlsruhe (1986).
7. S. GEGGUS, G. ADRIAN, H. APPEL, H. HAFFNER, AND B. KANELLAKOPULOS, *Hyperfine Interact.* **28,** 585 (1986).
8. L. SODERHOLM, *J. Less-Common Met.* **133,** 77 (1987).
9. M. BICKEL, S. GEGGUS, G. ADRIAN, H. APPEL, H. HAFFNER, AND B. KANELLAKOPULOS, unpublished.
10. J. B. GOODENOUGH AND J. M. LONGO, "Landolt Bornstein, Numerical and Technical Data," Vol. III, Part 4a, p. 131, Springer Pub., New York (1970).
11. A. J. JACOBSON, B. C. TOFIELD, AND B. E. F. FENDER, *Proc. 10th Rare Earth Res. Conf.* **1,** 194 (1973).
12. M. YOSHIMURA, T. NAKAMURA, AND T. SATA, *Chem. Lett.* **9,** 923 (1973).
13. G. BRAUER AND H. KRISTEN, *Z. Anorg. Allg. Chem.* **456,** 41 (1971).
14. S. A. BARRETT, A. J. JACOBSON, B. C. TOFIELD, AND B. E. F. FENDER, *Acta Crystallogr. Sect. B* **38,** 2775 (1982).
15. S. E. NAVE, R. G. HAIRE, AND P. G. HURAY, *Phys. Rev. B* **28,** 2317 (1983).
16. C. W. WILLIAMS, L. R. MORSS, AND I. K. CHOI, "Geochemical Behavior of Disposed Radioactive Waste" (G. S. Barney, J. D. Navratil, and W. W. Schultz, Eds.), Amer. Chem. Soc. Symp. Ser. No. 246, Amer. Chem. Soc., Washington, DC (1984).
17. L. SODERHOLM, L. R. MORSS, AND M. F. MOHAR, *J. Less-Common Met.* **127,** 131 (1987).
18. L. SODERHOLM AND H. RUMMENS, unpublished results.
19. B. C. TOFIELD, A. J. JACOBSON, AND B. E. F. FENDER, *J. Phys. C* **5,** 2887 (1972).
20. D. C. HARRIS AND TERRELL A. HEWSTON, *J. Solid State Chem.* **69,** 182 (1987).
21. A. J. JACOBSON, B. C. TOFIELD, AND B. E. F. FENDER, *Acta Crystallogr. Sect. B* **28,** 956 (1972).
22. S. GELLER, *J. Chem. Phys.* **24,** 1236 (1956).
23. J. T. LAST, *Phys. Rev.* **105,** 1740 (1957).
24. C. H. PERRY, B. N. KHANNA, AND G. RUPPRECHT, *Phys. Rev. A* **135,** 408 (1964).
25. J. B. MACCHESNEY, H. J. WILLIAMS, R. C. SHERWOOD, AND J. F. PORTER, *J. Chem. Phys.* **41**(10), 3177 (1964).
26. L. SODERHOLM AND J. E. GREEDAN, *Mater. Res. Bull.* **14,** 1449 (1979).
27. K. W. H. STEVENS, *Proc. Phys. Soc. (London) A* **65,** 209 (1952).
28. V. KAUFMAN AND J. SUGAR, *J. Res. Natl. Bur. Stand. Sect. A* **71,** 583 (1967).
29. S. KERN, C.-K. LOONG, AND G. H. LANDER, *Phys. Rev. B* **32**(5), 3051 (1985).
30. M. T. HUTCHINGS, *Solid State Phys.* **16,** 227 (1964).
31. A. J. FREEMAN AND R. E. WATSON, *Phys. Rev.* **127,** 2058 (1962).
32. R. W. WHITE, "Quantum Theory of Magnetism," Springer-Verlag, Berlin (1983).
33. C. J. BALLHAUSEN, "Ligand Field Theory," McGraw–Hill, New York (1962).
34. G. L. GOODMAN AND M. FRED, *J. Chem. Phys.* **30,** 849 (1959).
35. G. L. GOODMAN, Doctoral Dissertation, Harvard, Cambridge, MA (1959).
36. C. A. HUTCHISON AND B. WEINSTOCK, *J. Phys. Chem.* **32,** 56 (1960).
37. P. W. SELWOOD, "Magnetochemistry," Interscience, New York (1956).